IRIS AperTO

UNIVERSITÀ DEGLI STUDI DI TORINO

AperTO - Archivio Istituzionale Open Access dell'Università di Torino

Monocarboxylate transporter MCT1 promotes tumor metastasis independently of its activity as a lactate transporter

This is the author's manuscript

Original Citation:

Availability:

This version is available http://hdl.handle.net/2318/1661661 since 2018-10-29T14:53:18Z

Published version:

DOI:10.1158/0008-5472.CAN-17-0764

Terms of use:

Open Access

Anyone can freely access the full text of works made available as "Open Access". Works made available under a Creative Commons license can be used according to the terms and conditions of said license. Use of all other works requires consent of the right holder (author or publisher) if not exempted from copyright protection by the applicable law.

(Article begins on next page)

16 November 2026

Author Manuscript Published OnlineFirst on August 21, 2017; DOI: 10.1158/0008-5472.CAN-17-0764
Author manuscripts have been peer reviewed and accepted for publication but have not yet been edited.

Monocarboxylate transporter MCT1 promotes tumor metastasis independently of its activity as a lactate transporter

Valéry L Payen,[1] Myriam Y Hsu,[1] Kristin S Rädecke,[1] Elisabeth Wyart,[2] Thibaut Vazeille,[1] Caroline Bouzin,[3] Paolo E Porporato[1,2] and Pierre Sonveaux[1,*]

[1]Pole of Pharmacology, Institut de Recherche Expérimentale et Clinique (IREC), Université catholique de Louvain (UCL), Brussels, Belgium. [2]Department of Molecular Biotechnology and Health Sciences, University of Turin, Italy. [3]Imaging Platform, Institut de Recherche Expérimentale et Clinique (IREC), Université catholique de Louvain (UCL), Brussels, Belgium.

Corresponding author: Pierre Sonveaux, Pole of Pharmacology, Institut de Recherche Expérimentale et Clinique (IREC), Université catholique de Louvain (UCL), Avenue Emmanuel Mounier 52 box B1.53.09, 1200 Brussels, Belgium. Phone: +32 2 7645267; Fax: +32 2 764 5269; E-mail: pierre.sonveaux@uclouvain.be.

Running title: MCT1 promotes tumor metastasis

Keywords: Tumor metastasis, tumor metabolism, lactate, monocarboxylate transporter 1 (MCT1), nuclear factor-κB (NF-κB)

Financial support: This work was supported by a Starting Grant from the European Research Council (ERC No. 243188 TUMETABO) to P.S., Interuniversity Attraction Pole (IAP) grant #UP7-03 from the Belgian Science Policy Office (Belspo) to P.S., an Action de Recherche Concertée from the Communauté Française de Belgique (ARC 14/19-058) to P.S., the Belgian Fonds National de la Recherche Scientifique (F.R.S.-FNRS) to P.S., the Belgian Fondation contre le Cancer (Fundamental Research Grant #F86) to P.S., the Télévie to P.S., the Fonds Joseph Maisin to P.E.P. and P.S. and the Louvain Foundation to P.S.. P.S. is a Senior Research Associate and V.L.P. a PhD Fellow of the F.R.S.-FNRS.

Conflict of interest: The authors declare no potential conflicts of interest.

Note: Supplementary data for this article are available at Cancer Research Online (http://cancerres.aacrjournals.org/).

Abstract word count: 168/250
Total word count (without refs and legends): 4,538/5,000
Total #figures: 6/7
Total #ref: 50/50

Downloaded from cancerres.aacrjournals.org on September 20, 2017. © 2017 American Association for Cancer Research.

Author Manuscript Published OnlineFirst on August 21, 2017; DOI: 10.1158/0008-5472.CAN-17-0764
Author manuscripts have been peer reviewed and accepted for publication but have not yet been edited.

Abstract

Extracellular acidosis resulting from intense metabolic activities in tumors promotes cancer cell migration, invasion and metastasis. While host cells die at low extracellular pH, cancer cells resist, as they are well equipped with transporters and enzymes to regulate intracellular pH homeostasis. A low extracellular pH further activates proteolytic enzymes that remodel the extracellular matrix to facilitate cell migration and invasion. Monocarboxylate transporter MCT1 is a passive transporter of lactic acid that has attracted interest as a target for small molecule drugs to prevent metastasis. In this study, we present evidence of a function for MCT1 in metastasis beyond its role as a transporter of lactic acid. MCT1 activated transcription factor NF-κB to promote cancer cell migration independently of MCT1 transporter activity. While pharmacological MCT1 inhibition did not modulate MCT1-dependent cancer cell migration, silencing or genetic deletion of *MCT1 in vivo* inhibited migration, invasion and spontaneous metastasis. Our findings raise the possibility that pharmacological inhibitors of MCT1-mediated lactic acid transport may not effectively prevent metastatic dissemination of cancer cells.

Downloaded from cancerres.aacrjournals.org on September 20, 2017. © 2017 American Association for Cancer Research.

Author Manuscript Published OnlineFirst on August 21, 2017; DOI: 10.1158/0008-5472.CAN-17-0764
Author manuscripts have been peer reviewed and accepted for publication but have not yet been edited.

Introduction

Cancer cells deploy several strategies to survive and proliferate in poorly permissive tumor microenvironments characterized by hypoxia and nutrient deprivation. Among metabolic strategies, hypoxic/glycolytic cancer cells can cooperate with oxidative cancer cells by swapping glycolytic end-product lactic acid against blood-born glucose (1), and oxidative cancer cells can further obtain lactate by coopting stromal cell metabolism (2, 3). At the core of these metabolic relationships, oxidative cancer cells use lactate as preferential oxidative fuel to glucose, thus sparing glucose for glycolytic cells (1).

Lactate exchanges in cancer are governed by monocarboxylate transporters (MCTs) of the *SLC16* gene family that passively convey lactate and protons across the cell membrane (4). MCT1 and MCT4 are the main isoforms expressed by cancer cells (5). With a Km for lactate of 22-28 mM and a high turnover rate, hypoxia-inducible MCT4 is adapted for lactic acid export by glycolytic cells (6, 7). Comparatively, MCT1 has a lower 3.5–10 mM Km for lactate (4). Considering that the average concentration of lactate is ~10 mM in human solid tumors (8) and that oxidative cancer cells consume lactate (1), MCT1 is optimized for lactic acid uptake by these cells. However, as a passive transporter, MCT1 can operate bidirectionally and has also been reported to facilitate lactic acid export from cancer cells (9-12). The directionality of MCT1-driven lactic acid transport indeed depends on the gradient of lactate and protons membranes.

In growing tumors, functional characterization recently revealed that MCTs are not only gatekeepers of intercellular metabolic cooperation, but also important regulators of angiogenesis. Lactate that enters into oxygenated endothelial cells and oxidative cancer cells *via* MCT1 indeed promotes angiogenesis as it acts as a hypoxia-mimetic that

Downloaded from cancerres.aacrjournals.org on September 20, 2017. © 2017 American Association for Cancer Research.

Author Manuscript Published OnlineFirst on August 21, 2017; DOI: 10.1158/0008-5472.CAN-17-0764
Author manuscripts have been peer reviewed and accepted for publication but have not yet been edited.

activates transcription factors hypoxia-inducible factor-1 (HIF-1) and nuclear factor-κB (NF-κB), thereby stimulating the production of pro-angiogenic agents vascular endothelial growth factor (VEGF), basic fibroblast growth factor (bFGF) and interleukin-8 (IL-8) (13). Consequently, pharmacological MCT1 inhibitors have been proposed to simultaneously inhibit lactate exchanges and angiogenesis in tumors with limited side effects (5, 14), making of them particularly good candidate drugs for anticancer treatment. Hence, MCT1 inhibitor AZD3965 is currently tested in Phase I/II clinical trials in patients with prostate cancer, gastric cancer or diffuse large B cell lymphoma (ClinicalTrials.gov, NCT01791595).

Advanced stage tumors often undergo a metastatic switch, and metastatic dissemination strongly limits curative opportunities. Identifying treatments capable of preventing metastasis is, therefore, an urgent task. At least 3 lines of evidence suggest that lactate and MCTs, especially MCT1, promote tumor metastasis. First, analyses of primary tumor biopsies from patients revealed that high levels of lactate predict the likelihood of tumor metastasis (15-18). Second, MCT1 forms stable heterocomplexes with chaperon protein CD147/basigin (19), and CD147 promotes cancer cell invasion and metastasis (20). Third, we and others recently reported that MCT1 stimulates the migration and invasion of (glucose-starved) cancer cells towards serum or glucose (12, 21-23). Gray *et al.* (24) further proposed that MCT1 could facilitate cancer cell migration independently of its transporter activity based on the observation that silencing *MCT1* with a shRNA inhibited the *in vitro* scattering of prostate cancer cells stimulated with epithelial growth factor (EGF) or hepatocyte growth factor (HGF), whereas AZD3965 used at concentrations up to 10 μM did not. In this context, we analyzed the contribution of MCT1 to the tumor metastasis. We report that MCT1 activates NF-κB to promote

Downloaded from cancerres.aacrjournals.org on September 20, 2017. © 2017 American Association for Cancer Research.

Author Manuscript Published OnlineFirst on August 21, 2017; DOI: 10.1158/0008-5472.CAN-17-0764
Author manuscripts have been peer reviewed and accepted for publication but have not yet been edited.

cancer cell migration independently of its transport activity. Consequently, *MCT1* silencing or its genetic deletion inhibited cancer cell migration and invasion *in vitro* and spontaneous tumor metastasis *in vivo*.

Downloaded from cancerres.aacrjournals.org on September 20, 2017. © 2017 American Association for Cancer Research.

Author Manuscript Published OnlineFirst on August 21, 2017; DOI: 10.1158/0008-5472.CAN-17-0764
Author manuscripts have been peer reviewed and accepted for publication but have not yet been edited.

Materials and Methods

Cell culture and reagents

Superinvasive SiHa-F3 and mitochondria-deficient SiHa ρ0 cells were generated from wild-type SiHa human cervix adenocarcinoma cells (obtained in 2010 from ATCC) as in reference (25). 4T1 mouse mammary carcinoma cells were a kind gift of Fred R. Miller (Karmanos Cancer Institute, Detroit, MI) in 2011. Cells were routinely cultured in DMEM containing 4.5 g/L (25 mM) glucose, GlutaMAX (Gibco), and 10% FBS (Sigma) in a humidified atmosphere at 37°C, 5% CO_2. SiHa ρ0 further received 50 ng/mL of uridine (Sigma) and 1 mM of sodium pyruvate (Gibco). Cells were used from passage 2 to passage 15 after thawing and regularly tested for mycoplasma using the MycoAlert detection kit (Lonza). MCT1 inhibitors AR-C155858 (Tocris) and AZD3965 (Selleckchem) were dissolved in DMSO. Tumor necrosis factor α (TNFα) was from Miltenyi, tetradecanoyl phorbol myristate acetate (TPA) from Sigma-Aldrich and NF-κB inhibitor BMS-345541 from Tocris. Unless stated otherwise, assays were performed in culture medium.

Transfection and infection

For luciferase expression, 4T1 were infected with lentiviruses carrying the luciferase sequence (Addgene 21471) following a previously disclosed protocol (25).

For *MCT1* silencing with small interfering RNAs (siRNAs), SiHa cells were transfected with siCTR (Qiagen 1027281) or siMCT1 (Qiagen AAG AGG CUG ACU UUU CCA AAU) as previously described (26) and assayed 48 h after transfection.

Downloaded from cancerres.aacrjournals.org on September 20, 2017. © 2017 American Association for Cancer Research.

Author Manuscript Published OnlineFirst on August 21, 2017; DOI: 10.1158/0008-5472.CAN-17-0764
Author manuscripts have been peer reviewed and accepted for publication but have not yet been edited.

For *MCT1* silencing with short hairpin RNAs (shRNAs), cells were infected with lentiviruses as previously described (27). shRNAs targeted human *MCT1* (shMCT1; Thermo Scientific TRCN0000038339) or mouse *MCT1* (shMCT1a; Thermo Scientific TRCN0000079545 and shMCT1b; Thermo Scientific TRCN0000079547). shCTR- and shMCT1-expressing SiHa-F3 cells were further infected with lentiviruses carrying green fluorescent protein (EGFP, Addgene 12252) or red fluorescent tdTomato (Addgene 21374), and the cells were FACS-sorted on an Aria III cell sorter (BD Biosciences). In rescue experiments, mouse 4T1-shMCT1a cells were transfected with human wild-type *MCT1* ($hMCT1^+$) cDNA using pCMV6/Entry-mct1 plasmid (OriGene), and selected with G418 (400 µg/mL).

For *MCT1* deletion, SiHa-CRISPR-MCT1 cells were produced using Sigma LentiCRISPR (Target sequence: GTATAGTCATGATTGTTGGTGG) (27), and selected using puromycin. In rescue experiments, SiHa-CRISPR-MCT1 cells were transfected as in reference (28) with Cas9-resistant human *MCT1* cDNA (3 conservative point mutations in target sequence: GTATAGTCATGATaGTgGGTGG) that was mutated/inactivated for proton- and lactate-binding sites (38K>R, 302D>R, 306R>D) (29) using pEX-K4-MCT1 plasmid (Eurofins). This mutant transgene was named $hMCT1^-$. pEGFP-c1 (Clontech) was used as a negative and transfection-quality control. Cells were used 96 h after transfection.

Western blotting

Cells were lysed in RIPA buffer containing inhibitor cocktails of proteases (Sigma) and phosphatases (PhosSTOP; Roche), and western blotting was performed as previously described (30). Primary antibodies were: rabbit antibodies against MCT1 (Chemicon

Downloaded from cancerres.aacrjournals.org on September 20, 2017. © 2017 American Association for Cancer Research.

Author Manuscript Published OnlineFirst on August 21, 2017; DOI: 10.1158/0008-5472.CAN-17-0764
Author manuscripts have been peer reviewed and accepted for publication but have not yet been edited.

#AB3538P), human MCT4 (Chemicon #AB3316P), mouse MCT4 (Santa-Cruz #sc-50329), p65 (Cell Signaling #8242), p-Ser536-p65 (Cell Signaling #3033); and mouse antibodies against human CD147 (BD Biosciences #555961), HSP-90 (BD Biosciences #610419), and β-actin (Sigma #A5441). Secondary antibodies were HRP-coupled goat anti-rabbit and anti-mouse (Jackson).

Cell viability and proliferation assay

At Day 0, 2,000 SiHa or 4,000 4T1 cells per well were seeded in 96-well plates. Images were daily captured on a SpectraMax miniMax300 imaging cytometer (Molecular Devices) and analyzed with the Softmax Pro software (Molecular Devices). Results were normalized to cell number at Day 0.

Cell migration and invasion

Migration was first assayed using a scratch test following a previously disclosed protocol (31). Cells in culture medium containing 0.5 µg/mL of proliferation inhibitor mitomycin C were allowed to migrate for 48 h in a humidified atmosphere at 37°C, 5% CO_2. To measure scratch closure, images were captured every 4 h on an Axio Observer.Z1 time lapse microscope (Zeiss). Data were analyzed using ImageJ (NIH).

For transwell assays, cell migration was tested on a multiwell chemotaxis chamber (Neuro Probe) or using transwell inserts (Corning #353097). Briefly, 50,000 cells in serum-free culture medium were seeded in the upper chamber of each well, and FBS 0.15% was used as a chemoattractant in the lower chamber. Invasion was assayed using transwell inserts (regular Corning #353097 and Fluoroblok Corning #351152) coated with growth factor-reduced and phenol red-free Matrigel (Corning #356231)

Downloaded from cancerres.aacrjournals.org on September 20, 2017. © 2017 American Association for Cancer Research.

Author Manuscript Published OnlineFirst on August 21, 2017; DOI: 10.1158/0008-5472.CAN-17-0764
Author manuscripts have been peer reviewed and accepted for publication but have not yet been edited.

diluted 1:10 in PBS. Briefly, 100,000 cells in serum-free culture medium were seeded in the upper chamber of each well, and FBS 5% was used as a chemoattractant in the lower chamber. Cells were allowed to migrate for 16 h or to invade for 24 h in a humidified atmosphere at 37°C, 5% CO_2. Migrated/invaded cells were then fixed with methanol. Non-fluorescent cells were stained with a 0.023% crystal violet solution. Images were captured on an AxioVert microscope equipped with an AxioCam-MRc camera (Zeiss), and cells were counted using ImageJ.

Clonogenicity

Clonogenicity was tested on noble agar 0.33% (Sigma). Colonies were allowed to grow for 14 days before staining with a saturated MTT solution (Calbiochem) diluted in PBS. Pictures were taken under a Stemi 2000-C dissection microscope (Zeiss), and colonies were counted using ImageJ.

Metabolic assays

Glucose consumption and lactate release were determined with enzymatic assays on a CMA 600 Microdialysis analyzer (CMA Microdialysis) following manufacturer's instructions. Experimental conditions were: 150,000 SiHa cells/well for 24 h in 0.5 mL of culture medium and 100,000 4T1 cells/well for 24 h in 1 mL of culture medium. Results were normalized to total protein content (Bradford).

Intracellular lactate concentration was determined on adherent cells in 96-well plates that were incubated for 30 min in 100 µL of culture medium, washed with PBS and lysed *in situ.* Samples were analyzed using a lactate bioluminescent detection assay kit (kind gift from Promega) according to manufacturer's instructions.

Downloaded from cancerres.aacrjournals.org on September 20, 2017. © 2017 American Association for Cancer Research.

Author Manuscript Published OnlineFirst on August 21, 2017; DOI: 10.1158/0008-5472.CAN-17-0764
Author manuscripts have been peer reviewed and accepted for publication but have not yet been edited.

Bioluminescence was measured with a GloMax 96 Microplate luminometer (Promega). Data were normalized to cell number.

Oxygen consumption rate (OCR) and extracellular acidification rate (ECAR) were measured on 20,000 cells/well using a Seahorse XF96 analyzer (Agilent) with a combination of XF cell mito stress kit (Agilent) and 2-deoxy-*D*-glucose (2DG, Sigma). Basal mitochondrial OCR is the difference between initial OCR and OCR after inhibition of the electron transport chain (ETC) by rotenone (0.5 µM) and antimycin A (0.5 µM). Maximal mitochondrial OCR is the difference between OCR after injection of uncoupler FCCP (1 µM) and OCR after injection of rotenone and antimycin A. Glycolytic ECAR is the difference between initial ECAR and ECAR after injection of 2DG (100 mM). All assays were performed in unbuffered serum-free DMEM supplemented with 10 mM *D*-glucose and 2 mM *L*-glutamine, pH 7.4. Results were normalized to cell number or total protein content (Bradford).

Determination of intracellular and perimembranous pH

Intracellular pH (pHi) was determined on 20,000 cells with 5,6-carboxy-SNARF-1-acetomethylester (SNARF-AM, Molecular Probes) and pH at the outer side of the cell membrane with *N*-(fluorescein-5-thiocarbamoyl)-1,2-dihexadecanoyl-*sn*-glycero-3-phosphoethanolamine (fluorescein-DHPE, Molecular Probes), as previously reported (32). Calibration for pHi was performed on carboxy-SNARF-1-loaded cells treated with potassium/proton ionophore nigericin (2.5 µM) and hyperpotassic solutions at pH values ranging from 6.6 to 8.0. Calibration for extracellular membrane pH was performed with fluorescein-DHPE in solutions at pH 4.9 to 9.2. Fluorescence was measured on a SpectraMax miniMax300 imaging cytometer.

Downloaded from cancerres.aacrjournals.org on September 20, 2017. © 2017 American Association for Cancer Research.

Author Manuscript Published OnlineFirst on August 21, 2017; DOI: 10.1158/0008-5472.CAN-17-0764
Author manuscripts have been peer reviewed and accepted for publication but have not yet been edited.

In vivo experiments

All *in vivo* experiments were conducted under approval of the Université catholique de Louvain (UCL) authorities (*Comité d'Ethique Facultaire pour l'Expérimentation Animale*) according to national animal care regulations (authorization #2012/UCL/MD/005).

For spontaneous metastasis assays, 200,000 luciferase-expressing 4T1 were subcutaneously injected in the flank of 7 weeks-old syngeneic BALB/cJRj female mice (Janvier). Primary tumor growth was regularly measured over time with a caliper, and tumor volume was calculated as previously described (33). Primary tumors were surgically resected between day 24 and 31, *i.e.*, when their average diameter reached 10 mm. They were embedded in paraffin, and two 5 µm-thick central sections for each tumor were stained with hematoxylin and eosin (H&E) and immunostained for cleaved caspase 3 (Cell signaling #9661) or Ki-67 (Cell signaling #12202). All mice were sacrificed at day 38 by cervical dislocation. Ten minutes before sacrifice, mice were i.p. injected with 0.15 mg/g bodyweight of luciferin (PerkinElmer). Five minutes after sacrifice, lungs were inflated with a 15 mg/mL luciferin solution and bathed in the same solution for 5 min. Chemiluminescence was acquired on harvested lungs during 4 min with a Xenogen IVIS 50 bioluminescence imaging system (PerkinElmer), and quantified with the Living Image software (PerkinElmer). Lungs were further examined under a Stemi 2000-C dissection microscope to count surface metastases. They were then embedded in paraffin, and 5 µm-thick lung sections (2 different plans for each lobe of each animal) were stained with H&E. All slices were scanned with a SCN400 bright field slide scanner (Leica) at 20x magnification. Quantitative data were obtained with the Tissue IA software (Leica).

Downloaded from cancerres.aacrjournals.org on September 20, 2017. © 2017 American Association for Cancer Research.

Author Manuscript Published OnlineFirst on August 21, 2017; DOI: 10.1158/0008-5472.CAN-17-0764
Author manuscripts have been peer reviewed and accepted for publication but have not yet been edited.

Statistics

Except in dot plots that show individual values and group averages, all data show means ± SEM (error bars are sometimes smaller than symbols). *n* indicates the total number of replicates. Student's *t* test, one-way ANOVA with Dunnett's or Bonferroni's post-hoc tests, and two-way ANOVA on matched values with Bonferroni's post-hoc test were applied where indicated. $P < 0.05$ was considered to be statistically significant.

Downloaded from cancerres.aacrjournals.org on September 20, 2017. © 2017 American Association for Cancer Research.

Author Manuscript Published OnlineFirst on August 21, 2017; DOI: 10.1158/0008-5472.CAN-17-0764
Author manuscripts have been peer reviewed and accepted for publication but have not yet been edited.

Results

MCT1 promotes cancer cell migration and invasion

To address the contribution of MCT1 to cancer metastasis, we used human SiHa cervix squamous carcinoma cells and 4T1 mouse mammary carcinoma cells. Both cell lines express MCT1 (**Fig. S1A**).

In the absence of exogenous lactate except from serum, *MCT1* silencing using siMCT1 or shMCT1 and *MCT1* deletion using a CRISPR-Cas9 strategy (**Fig. S1A**) did not affect SiHa cell count (**Fig. S1B**) but reduced SiHa cell migration (**Fig. 1A**) and invasion (**Fig. 1B**) towards serum by about 50 to 80%. A scratch test further revealed that SiHa cell migration was sustainably inhibited by shMCT1 over 48 h (**Fig. S1C**). Thus, SiHa cell migration and invasion were inhibited upon *MCT1* silencing or deletion. Of note, shMCT1, but not CRISPR-MCT1, was associated with an increase in MCT4 expression (**Fig. S1A**). Expression of CD147/basigin was unchanged. Of further note, providing lactate to SiHa cells barely affected their migratory activity. In transwells, 20 mM of lactate (34) delivered in the upper compartment significantly reduced SiHa migration by about 10%, and lactate did not act as a chemoattractant (**Fig. S1D**).

That MCT1 promotes cancer cell migration was verified using 4T1 mouse mammary carcinoma cells (see metabolic characterization below). *MCT1* silencing with shMCT1a or shMCT1b (**Fig. S1A**) did not affect clonogenicity (**Fig. S1E**) but reduced 4T1 cell migration by about 65% (**Fig. 1C**) and invasion by about 40% (**Fig. 1D**). There was no increase in MCT4 expression upon *MCT1* silencing (**Fig. S1A**).

Downloaded from cancerres.aacrjournals.org on September 20, 2017. © 2017 American Association for Cancer Research.

Author Manuscript Published OnlineFirst on August 21, 2017; DOI: 10.1158/0008-5472.CAN-17-0764
Author manuscripts have been peer reviewed and accepted for publication but have not yet been edited.

Suppressing MCT1 expression decreases lactic acid efflux from cancer cells

Because cancer cell metabolism can impact migration, invasion and metastasis (35), we characterized the metabolic consequences of *MCT1* silencing/deletion in SiHa and 4T1 cells in the same conditions as in migration and invasion assays.

In SiHa cells, shMCT1 did not modify glucose consumption (**Fig. 2A**) but reduced lactate release (**Fig. 2B**), and lactate accumulated intracellularly (**Fig. S2A**). shMCT1 further decreased the extracellular acidification rate (ECAR) directly attributable to glycolysis (**Fig. 2C**), whereas intracellular pH slightly decreased (**Fig. S2B**). pH at the outer side of the cell membrane was less acidic (**Fig. S2C**). Similarly, deleting *MCT1* using CRISPR-Cas9 resulted in decreased lactate release (**Fig. 2B**) and decreased glycolytic ECAR (**Fig. 2C**) with unchanged glucose consumption (**Fig. 2A**). Lactate accumulated intracellularly (**Fig. S2A**). Thus, inhibiting MCT1 expression decreased the glycolytic efficiency of SiHa cells. Oxidative activity was measured on a Seahorse XF96 oximeter. Compared to shCTR, shMCT1 did not modify the basal OCR of SiHa cells or their maximal respiratory capacity (**Fig. 2D-F**). In contrast, both parameters increased in SiHa-CRISPR-MCT1 compared to wild-type SiHa cells (**Fig. 2D-F**).

Metabolic characterization was also performed for 4T1 cells. Compared to shCTR, shMCT1a and shMCT1b decreased 4T1 glucose consumption (**Fig. 2G**) and lactate release (**Fig. 2H**), which was associated to a decreased glycolytic ECAR (**Fig. 2I**). Basal and maximal OCR increased (**Fig. 2J**), especially with shMCT1b that was more efficient than shMCT1a to repress MCT1 protein expression in these cells (**Fig. S1A**).

Downloaded from cancerres.aacrjournals.org on September 20, 2017. © 2017 American Association for Cancer Research.

Author Manuscript Published OnlineFirst on August 21, 2017; DOI: 10.1158/0008-5472.CAN-17-0764
Author manuscripts have been peer reviewed and accepted for publication but have not yet been edited.

The transporter activity of MCT1 does not participate in MCT1-dependent cancer cell migration and invasion

An acidic environment promotes cancer cell migration, invasion and metastasis (35). Because as a passive transporter MCT1 can transport lactic acid bidirectionally, we investigated whether MCT1 activity is involved in the prometastatic phenotype. Inhibition of MCT1 with increasing doses of AR-C155858 (27) or 10 µM of AZD3965 (24) did not significantly modify glucose consumption (**Fig. 3A**) but reduced lactate release (**Fig. 3B**) by SiHa cells, and lactate accumulated intracellularly (**Fig. S3A**). AR-C155858 also reduced proton export by the cells (**Fig. 3C**) and promoted intracellular acidification (**Fig. S3B**). At 10 µM, it did not affect the OCR of the cells (**Fig. S3C**) or their number (**Fig. S3D**). However, despite the striking similarity of the metabolic effects seen with *MCT1* suppression and its inhibition, AR-C155858 did not inhibit SiHa cell migration (**Fig. 3D**) or invasion (**Fig. 3E**). AZD3965 (10 µM) did not impair SiHa cell migration (**Fig. 3D**). Of note, we verified that neither AR-C155858 nor AZD3965 altered MCT1, MCT4 and CD147 expression in the cells (**Fig. S3E**).

In 4T1 cells, AR-C155858 was used at a 10 nM concentration that did not affect cell number (**Fig. S3F**) but efficiently decreased glucose consumption (**Fig. 3F**) and lactic acid release (**Fig. 3G** and **Fig. S3G**). AR-C155858 did not affect 4T1 cell migration (**Fig. 3H**) or invasion (**Fig. 3I**). MCT1 was also re-expressed in 4T1-shMCT1a cells, and we opted for a human sequence resistant to the anti-mouse shRNA ($hMCT1^{+}$), which restored 4T1 cell migration (**Fig. 3J**).

To demonstrate that MCT1 promotes cancer cell migration independently of its transporter activity, we generated a Cas9-resistant and transport-inactive (38K>R, 302D>R, 306R>D) (29) version of the transporter ($hMCT1^{-}$). Expression of $hMCT1^{-}$ in

Downloaded from cancerres.aacrjournals.org on September 20, 2017. © 2017 American Association for Cancer Research.

Author Manuscript Published OnlineFirst on August 21, 2017; DOI: 10.1158/0008-5472.CAN-17-0764
Author manuscripts have been peer reviewed and accepted for publication but have not yet been edited.

SiHa-CRISPR-MCT1 cells restored migration (**Fig. 3K**). EGFP was used in control experiments, evidencing that about 50% of the cells were efficiently transfected (**Fig. S3H**).

Highly invasive cancer cells have a high MCT1 expression that promotes their migration and invasion

To further analyze the relationship between MCT1 expression and the prometastatic phenotype, we used SiHa-F3 and SiHa-ρ0 cells, which have been reported to be more migratory and invasive than SiHa-WT (25).

SiHa-F3 had increased MCT1 expression compared to SiHa-WT, whereas MCT4 expression was decreased and CD147 expression was unmodified (**Fig. 4A**). Compared to SiHa-WT, SiHa-F3 cells had increased glucose consumption (**Fig. S4A**) and lactate release (**Fig. S4B**), increased glycolytic ECAR (**Fig. S4C**) and increased basal OCR (**Fig. S4D**). They were more migratory than SiHa-WT cells (**Fig. 4B** and **Fig. S4E**). Conversely, silencing *MCT1* with shMCT1 in SiHa-F3 cells (**Fig. 4A**) decreased lactate release (**Fig. S4B**) and increased cell respiration (**Fig. S4D**). shMCT1, but not AR-C155858, significantly decreased SiHa-F3 cell migration and invasion (**Fig. 4B-C** and **Fig. S4E**).

Similarly, SiHa-ρ0 cells expressed more MCT1 compared to parental cells (**Fig. 4D**). Their *in vitro* migration and invasion was almost fully inhibited upon *MCT1* silencing (**Fig. 4E**).

Downloaded from cancerres.aacrjournals.org on September 20, 2017. © 2017 American Association for Cancer Research.

Author Manuscript Published OnlineFirst on August 21, 2017; DOI: 10.1158/0008-5472.CAN-17-0764
Author manuscripts have been peer reviewed and accepted for publication but have not yet been edited.

MCT1 expression, but not its transport activity, triggers NF-κB in cancer cells

We next sought to identify a mechanism through which MCT1 expression could control cancer cell migration independently of its activity as a transporter. Based on a previous report by Zhao *et al.* (36), we focused on transcription factor NF-κB. Compared to SiHa-WT, SiHa-F3 and SiHa-ρ0 cells had a higher phospho-Ser536-p65/total p65 ratio (**Fig. S5A**). Conversely, both SiHa-shMCT1 and SiHa-CRISPR-MCT1 had a decreased phospho-Ser536-p65 (human sequence)/total p65 ratio than control cells (**Fig. 5A**). Upstream of NF-κB pathway, *MCT1* deletion decreased IκKα but not IκKβ expression (**Fig. 5B**). Similarly, the phospho-Ser536-p65/total p65 ratio was decreased in 4T1 cells expressing shMCT1a or shMCT1b (**Fig. 5C**) and restored when 4T1-shMCT1 cells expressed $hMCT1^{+}$ (**Fig. S5B**). Of note, expression of mutated/inactivated $hMCT1^{-}$ in SiHa-CRISPR-MCT1 cells also increased p65 Ser536-phosphorylation (**Fig. S5C**), but cellular stress induced by the transfection procedure had a confounding effect.

Because changes in MCT1 expression but not its pharmacological inhibition by AR-C155858 or AZD3965 (**Fig. S5D**) influenced p65 phosphorylation, we tested whether NF-κB activation was sufficient to resume MCT1-deficent cell migration. NF-κB activation by TNFα or TPA (**Fig. S5E**) restored SiHa-CRISPR-MCT1 cell migration (**Fig. 5D**), and this effect was fully blocked by BMS-345541, a highly specific NF-κB inhibitor (37) (**Fig. S5E**). NF-κB inhibition and *MCT1* deletion had no additive antimigratory effects (**Fig. 5E**), which, together with the above data, indicated that NF-κB acts downstream of MCT1 to control cancer cell migration.

Downloaded from cancerres.aacrjournals.org on September 20, 2017. © 2017 American Association for Cancer Research.

Author Manuscript Published OnlineFirst on August 21, 2017; DOI: 10.1158/0008-5472.CAN-17-0764
Author manuscripts have been peer reviewed and accepted for publication but have not yet been edited.

MCT1 silencing inhibits spontaneous 4T1 breast cancer metastasis to the lungs

SiHa cells are only weakly metastatic in SCID mice (38). To evaluate the contribution of MCT1 expression to metastasis, we therefore used the 4T1 model where primary tumors spontaneously metastasize to the lungs of immunocompetent syngeneic mice (39). Luciferase-expressing 4T1-shCTR, 4T1-shMCT1a and 4T1-shMCT1b cells generated subcutaneous primary tumors with similar growth rates (**Fig. S6A**), necrotic cores, and apoptotic and proliferative fractions (**Fig. S6B**). However, *MCT1* silencing strongly decreased lung metastasis detected by *ex vivo* bioluminescence (**Fig. 6A**) and direct counts (**Fig. 6B**). These data were confirmed by histological analysis showing fewer (**Fig. 6C** *left*) and smaller (**Fig. 6C** *right*) metastases per total lung area in 4T1-shMCT1a and 4T1-MCT1b compared to 4T1-shCTR tumor-bearing mice.

Downloaded from cancerres.aacrjournals.org on September 20, 2017. © 2017 American Association for Cancer Research.

Author Manuscript Published OnlineFirst on August 21, 2017; DOI: 10.1158/0008-5472.CAN-17-0764
Author manuscripts have been peer reviewed and accepted for publication but have not yet been edited.

Discussion

This study aimed to clarify the contribution of MCT1 to cancer metastasis. We report that MCT1 promotes cancer cell migration and invasion independently of its activity as a transporter. Consequently, *MCT1* silencing or deletion, but not its pharmacological inhibition, repressed these phenotypes. Silencing *MCT1* further inhibited spontaneous metastatic dissemination in mice.

Since its identification as a transporter of lactic acid in cancer cells in 1994 (40) and in tumors in 2001 (41), MCT1 expression has been reported in a wide variety of human cancers, including head and neck, breast, lung, stomach, colon, bladder, prostate and cervix cancers, as well as gliomas (see references in (5)). Its transporter activity has been positively linked to the metabolic capability of cancer cells to switch substrates depending on their local bioavailability (5) and to tumor angiogenesis (13). However, to our knowledge and despite converging clues (12, 21-24, 36), there was no experimental demonstration that MCT1 contributes to tumor metastasis *in vivo*. The closest related study is probably that of Zhao *et al.* (36) who claimed that downregulation of MCT1 expression inhibits tumor metastasis, but these authors did not perform any *in vivo* experiments. Our demonstration that MCT1 promotes spontaneous tumor metastasis in immunocompetent mice thus confirms these previous hypothetical clues. Together with our precedent observations, it reveals that MCT1 facilitates three main strategies displayed by cancer cells in harsh microenvironmental conditions: to adapt to the environment (metabolic plasticity), to modify the environment (angiogenesis) and to leave the environment (migration, invasion and metastasis). Thus, high MCT1 expression facilitates cancer cell migration, invasion and metastasis. This characteristic

Downloaded from cancerres.aacrjournals.org on September 20, 2017. © 2017 American Association for Cancer Research.

Author Manuscript Published OnlineFirst on August 21, 2017; DOI: 10.1158/0008-5472.CAN-17-0764
Author manuscripts have been peer reviewed and accepted for publication but have not yet been edited.

is shared by different cancer cell types, including superinvasive SiHa-F3 and SiHa-ρ0 cervix adenocarcinoma cells that depend on high MCT1 expression for migration and invasion (this study) and clinical non‑small cell lung carcinomas (42) where metastatic lesions express higher levels of MCT1 than primary tumors. The latter observation further indicates that MCT1 could contribute to the growth of established metastases.

As a passive transporter, MCT1 can operate bidirectionally, which explains why it facilitated lactic acid export from SiHa and 4T1 cells in our experimental conditions. Accordingly, MCT1-deficient cells had a reduced capacity to acidify culture medium in general and the outer side of the cell membrane in particular. Generally, extracellular acidification triggers cell invasion by promoting protease activity and altering cellular adhesion (35, 43), but MCT1 turned out not to be an essential contributor to pH-dependent invasion. Indeed, while MCT1 inhibitors AR-C155858 and AZD3965 effectively reduced lactic acid release by the cells, they did not inhibit migration and invasion even when used at doses higher than what can be safely achieved *in vivo*. This observation can be related to the presence of several other sources of acidity, including CO_2, as notably evidenced by experiments that showed that glycolysis-deficient cancer cells that produce negligible amounts of lactic acid are as effective as glycolysis-competent cells to lower extracellular pH down to 6.7 (44). Thus, in agreement with Gray *et al.* (24) but not with Izumi *et al.* (22) who used nonselective MCT inhibitors, we report that MCT1 promotes cancer cell migration and invasion independently of its transporter activity. In support of this conclusion, expression of a transport-inactivated version of MCT1 lacking proton- and lactate-binding sites in *MCT1*-deleted cancer cells rescued migration.

Downloaded from cancerres.aacrjournals.org on September 20, 2017. © 2017 American Association for Cancer Research.

Author Manuscript Published OnlineFirst on August 21, 2017; DOI: 10.1158/0008-5472.CAN-17-0764
Author manuscripts have been peer reviewed and accepted for publication but have not yet been edited.

Mechanistically, based on previous observations (36), we confirmed that NF-κB is a downstream effector of MCT1 for cancer cell migration. Indeed, *MCT1* deletion reduced the expression of IκKα (a catalytically active constituent of the IκB kinase complex that normally triggers NF-κB activation) and reduced NF-κB activity and cell migration, and *MCT1* deletion and NF-κB inhibition had no additive effects on inhibition of cancer cell migration. Conversely, NF-κB activation restored the migration of *MCT1*-deficient cells, which was achieved either with pharmacological NF-κB activators or through MCT1 re-expression in deficient cells. Beyond its role as a transporter, MCT1 physically interacts with proteins, notably carbonic anhydrase II (CAII) (45), hyaluronan receptor CD44 (46) and CD147 (19). While cytosolic CAII regulates MCT1 transporter activity (47) and CD44 is a stem cell marker, transmembrane glycoprotein CD147, also known as extracellular matrix metalloproteinase inducer (EMMPRIN), is well-known to promote tumor metastasis (48). Interestingly, through a yet unknown mechanism, CD147 has been reported to activate NF-κB in cardiomyocytes (49) and in fibroblasts (50). Because interaction mutually stabilizes both proteins at the cell membrane, it would have been tempting to propose that MCT1-CD147 complexes could promote cancer cell migration and invasion through CD147-dependent NF-κB activation. However, CD147 expression was not altered in our MCT1-defective cell models, most probably because CD147 interacts with other proteins at the cell membrane, notably MCT4 (19). Thus, how MCT1 expression represses IκKα expression and activates NF-κB in cancer cells independently of lactate fluxes remains an open question. Hypotheses that merit to be addressed relate to the turnover rate of CD147 in *MCT1*-deficient cells, as the extracellular domain of CD147 has been proposed to control IκB kinase expression (50) (of which IκKα is a constituent) and to the possibility that MCT1 itself would initiate

Downloaded from cancerres.aacrjournals.org on September 20, 2017. © 2017 American Association for Cancer Research.

Author Manuscript Published OnlineFirst on August 21, 2017; DOI: 10.1158/0008-5472.CAN-17-0764
Author manuscripts have been peer reviewed and accepted for publication but have not yet been edited.

intracellular signaling through yet unknown protein-protein interaction(s). MCT1 could also further trigger NF-κB-independent pathways to promote cancer cell migration.

Conclusively, MCT1 activates NF-κB independently of its transporter activity, which promotes cancer cell migration, invasion and metastasis. We therefore believe that MCT1 inhibitors do not have the potential to achieve a clinical prevention of tumor metastasis, which of course does not impact their therapeutic interest as antimetabolic and anti-angiogenic drugs in established (primary and secondary) tumors.

Downloaded from cancerres.aacrjournals.org on September 20, 2017. © 2017 American Association for Cancer Research.

Author Manuscript Published OnlineFirst on August 21, 2017; DOI: 10.1158/0008-5472.CAN-17-0764
Author manuscripts have been peer reviewed and accepted for publication but have not yet been edited.

Acknowledgements

Authors thank Fred R. Miller (B.A. Karmanos Cancer Institute, Detroit, MI, USA) for the kind gift of the 4T1 cells; Marylène Focant (Promega) for the kind gift of lactate bioluminescent detection assay kits; Vincent F. Van Hée, Emilia Turco, Jean-François Toubeau, Marie-Christine Many and Lucie Brisson for scientific input and discussions; and Morgane Tardy, Chantal Fregimilicka, Michèle De Beukelaer, Catherine Lombard and Joachim Ravau for excellent technical support. P.E.P and P.S. are co-last authors.

Downloaded from cancerres.aacrjournals.org on September 20, 2017. © 2017 American Association for Cancer Research.

Author Manuscript Published OnlineFirst on August 21, 2017; DOI: 10.1158/0008-5472.CAN-17-0764
Author manuscripts have been peer reviewed and accepted for publication but have not yet been edited.

References

(1) Sonveaux P, Vegran F, Schroeder T, Wergin MC, Verrax J, Rabbani ZN, *et al.* Targeting lactate-fueled respiration selectively kills hypoxic tumor cells in mice. *J Clin Invest* **2008**;118:3930–42.

(2) Pavlides S, Whitaker-Menezes D, Castello-Cros R, Flomenberg N, Witkiewicz AK, Frank PG, *et al.* The reverse Warburg effect: aerobic glycolysis in cancer associated fibroblasts and the tumor stroma. *Cell Cycle* **2009**;8:3984–4001.

(3) Fiaschi T, Marini A, Giannoni E, Taddei ML, Gandellini P, De Donatis A, *et al.* Reciprocal metabolic reprogramming through lactate shuttle coordinately influences tumor-stroma interplay. *Cancer Res* **2012**;72:5130–40.

(4) Halestrap AP, Wilson MC. The monocarboxylate transporter family--role and regulation. *IUBMB Life* **2012**;64:109–19.

(5) Perez-Escuredo J, Van Hee VF, Sboarina M, Falces J, Payen VL, Pellerin L, *et al.* Monocarboxylate transporters in the brain and in cancer. *BBA Mol Cell Res* **2016**;1863:2481–97.

(6) Dimmer KS, Friedrich B, Lang F, Deitmer JW, Broer S. The low-affinity monocarboxylate transporter MCT4 is adapted to the export of lactate in highly glycolytic cells. *Biochem J* **2000**;350 Pt 1:219–27.

(7) Ullah MS, Davies AJ, Halestrap AP. The plasma membrane lactate transporter MCT4, but not MCT1, is up-regulated by hypoxia through a HIF-1alpha-dependent mechanism. *J Biol Chem* **2006**;281:9030–7.

(8) Walenta S, Schroeder T, Mueller-Klieser W. Lactate in solid malignant tumors: potential basis of a metabolic classification in clinical oncology. *Curr Med Chem* **2004**;11:2195–204.

(9) Le Floch R, Chiche J, Marchiq I, Naiken T, Ilk K, Murray CM, *et al.* CD147 subunit of lactate/H+ symporters MCT1 and hypoxia-inducible MCT4 is critical for energetics and growth of glycolytic tumors. *Proc Natl Acad Sci U S A* **2011**;108:16663–8.

(10) Polanski R, Hodgkinson CL, Fusi A, Nonaka D, Priest L, Kelly P, *et al.* Activity of the monocarboxylate transporter 1 inhibitor AZD3965 in small cell lung cancer. Clin *Cancer Res* **2014**;20:926–37.

(11) Morais-Santos F, Granja S, Miranda-Goncalves V, Moreira AH, Queiros S, Vilaca JL, *et al.* Targeting lactate transport suppresses in vivo breast tumour growth. *Oncotarget* **2015**;6:19177–89.

Downloaded from cancerres.aacrjournals.org on September 20, 2017. © 2017 American Association for Cancer Research.

Author Manuscript Published OnlineFirst on August 21, 2017; DOI: 10.1158/0008-5472.CAN-17-0764
Author manuscripts have been peer reviewed and accepted for publication but have not yet been edited.

(12) Miranda-Goncalves V, Granja S, Martinho O, Honavar M, Pojo M, Costa BM, *et al.* Hypoxia-mediated upregulation of MCT1 expression supports the glycolytic phenotype of glioblastomas. *Oncotarget* **2016**;7:46335–53.

(13) Payen VL, Brisson L, Dewhirst MW, Sonveaux P. Common responses of tumors and wounds to hypoxia. *Cancer J* **2015**;21:75–87.

(14) Dhup S, Dadhich RK, Porporato PE, Sonveaux P. Multiple biological activities of lactic acid in cancer: influences on tumor growth, angiogenesis and metastasis. *Curr Pharm Des* **2012**;18:1319–30.

(15) Walenta S, Salameh A, Lyng H, Evensen JF, Mitze M, Rofstad EK, *et al.* Correlation of high lactate levels in head and neck tumors with incidence of metastasis. *Am J Pathol* **1997**;150:409–15.

(16) Brizel DM, Schroeder T, Scher RL, Walenta S, Clough RW, Dewhirst MW, *et al.* Elevated tumor lactate concentrations predict for an increased risk of metastases in head-and-neck cancer. *Int J Radiat Oncol Biol Phys* **2001**;51:349–53.

(17) Schwickert G, Walenta S, Sundfor K, Rofstad EK, Mueller-Klieser W. Correlation of high lactate levels in human cervical cancer with incidence of metastasis. *Cancer Res* **1995**;55:4757–9.

(18) Walenta S, Wetterling M, Lehrke M, Schwickert G, Sundfor K, Rofstad EK, *et al.* High lactate levels predict likelihood of metastases, tumor recurrence, and restricted patient survival in human cervical cancers. *Cancer Res* **2000**;60:916–21.

(19) Wilson MC, Meredith D, Fox JE, Manoharan C, Davies AJ, Halestrap AP. Basigin (CD147) is the target for organomercurial inhibition of monocarboxylate transporter isoforms 1 and 4: the ancillary protein for the insensitive MCT2 is EMBIGIN (gp70). *J Biol Chem* **2005**;280:27213–21.

(20) Pan Y, He B, Song G, Bao Q, Tang Z, Tian F, *et al.* CD147 silencing via RNA interference reduces tumor cell invasion, metastasis and increases chemosensitivity in pancreatic cancer cells. *Oncol Rep* **2012**;27:2003–9.

(21) De Saedeleer CJ, Porporato PE, Copetti T, Perez-Escuredo J, Payen VL, Brisson L, *et al.* Glucose deprivation increases monocarboxylate transporter 1 (MCT1) expression and MCT1-dependent tumor cell migration. *Oncogene* **2014**;33:4060–8.

(22) Izumi H, Takahashi M, Uramoto H, Nakayama Y, Oyama T, Wang KY, *et al.* Monocarboxylate transporters 1 and 4 are involved in the invasion activity of human lung cancer cells. *Cancer Sci* **2011**;102:1007–13.

(23) Kong SC, Nohr-Nielsen A, Zeeberg K, Reshkin SJ, Hoffmann EK, Novak I, *et al.* Monocarboxylate Transporters MCT1 and MCT4 Regulate Migration and Invasion of Pancreatic Ductal Adenocarcinoma Cells. *Pancreas* **2016**;45:1036–47.

Downloaded from cancerres.aacrjournals.org on September 20, 2017. © 2017 American Association for Cancer Research.

Author Manuscript Published OnlineFirst on August 21, 2017; DOI: 10.1158/0008-5472.CAN-17-0764
Author manuscripts have been peer reviewed and accepted for publication but have not yet been edited.

(24) Gray AL, Coleman DT, Shi R, Cardelli JA. Monocarboxylate transporter 1 contributes to growth factor-induced tumor cell migration independent of transporter activity. *Oncotarget* **2016**;7:32695–706.

(25) Porporato PE, Payen VL, Perez-Escuredo J, De Saedeleer CJ, Danhier P, Copetti T, *et al.* A mitochondrial switch promotes tumor metastasis. *Cell Rep* **2014**;8:754–66.

(26) Perez-Escuredo J, Dadhich RK, Dhup S, Cacace A, Van Hee VF, De Saedeleer CJ, *et al.* Lactate promotes glutamine uptake and metabolism in oxidative cancer cells. *Cell Cycle* **2016**;15:72–83.

(27) Van Hee VF, Labar D, Dehon G, Grasso D, Gregoire V, Muccioli GG, *et al.* Radiosynthesis and validation of (+/-)-[18F]-3-fluoro-2-hydroxypropionate ([18F]-FLac) as a PET tracer of lactate to monitor MCT1-dependent lactate uptake in tumors. *Oncotarget* **2017**;8:24415–28.

(28) Halestrap AP, Price NT. The proton-linked monocarboxylate transporter (MCT) family: structure, function and regulation. *Biochem J* **1999**;343 Pt 2:281–99.

(29) Halestrap AP. The SLC16 gene family - structure, role and regulation in health and disease. *Mol Aspects Med* **2013**;34:337–49.

(30) Van Hée VF, Perez-Escuredo J, Cacace A, Copetti T, Sonveaux P. Lactate does not activate NF-kB in oxidative tumor cells. *Front Pharmacol* **2015**;6:228.

(31) Tamura M, Gu J, Matsumoto K, Aota S, Parsons R, Yamada KM. Inhibition of cell migration, spreading, and focal adhesions by tumor suppressor PTEN. *Science* **1998**;280:1614–7.

(32) Gillet L, Roger S, Besson P, Lecaille F, Gore J, Bougnoux P, *et al.* Voltage-gated sodium channel activity promotes cysteine cathepsin-dependent invasiveness and colony growth of human cancer cells. *J Biol Chem* **2009**;284:8680–91.

(33) De Saedeleer CJ, Copetti T, Porporato PE, Verrax J, Feron O, Sonveaux P. Lactate activates HIF-1 in oxidative but not in Warburg-phenotype human tumor cells. *PLoS ONE* **2012**;7:e46571.

(34) Goetze K, Walenta S, Ksiazkiewicz M, Kunz-Schughart LA, Mueller-Klieser W. Lactate enhances motility of tumor cells and inhibits monocyte migration and cytokine release. *Int J Oncol* **2011**;39:453–63.

(35) Payen VL, Porporato PE, Baselet B, Sonveaux P. Metabolic changes associated with tumor metastasis, part 1: tumor pH, glycolysis and the pentose phosphate pathway. *Cell Mol Life Sci* **2016**;73:1333–48.

(36) Zhao Z, Wu MS, Zou C, Tang Q, Lu J, Liu D, *et al.* Downregulation of MCT1 inhibits tumor growth, metastasis and enhances chemotherapeutic efficacy in

Downloaded from cancerres.aacrjournals.org on September 20, 2017. © 2017 American Association for Cancer Research.

Author Manuscript Published OnlineFirst on August 21, 2017; DOI: 10.1158/0008-5472.CAN-17-0764
Author manuscripts have been peer reviewed and accepted for publication but have not yet been edited.

osteosarcoma through regulation of the NF-kappaB pathway. *Cancer Lett* **2014**;342:150–8.

(37) Burke JR, Pattoli MA, Gregor KR, Brassil PJ, MacMaster JF, McIntyre KW, *et al.* BMS-345541 is a highly selective inhibitor of I kappa B kinase that binds at an allosteric site of the enzyme and blocks NF-kappa B-dependent transcription in mice. *J Biol Chem* **2003**;278:1450–6.

(38) Cairns RA, Hill RP. A fluorescent orthotopic model of metastatic cervical carcinoma. *Clin Exp Metastasis* **2004**;21:275–81.

(39) Aslakson CJ, Miller FR. Selective events in the metastatic process defined by analysis of the sequential dissemination of subpopulations of a mouse mammary tumor. *Cancer Res* **1992**;52:1399–405.

(40) Carpenter L, Halestrap AP. The kinetics, substrate and inhibitor specificity of the lactate transporter of Ehrlich-Lettre tumour cells studied with the intracellular pH indicator BCECF. *Biochem J* **1994**;304 (Pt 3):751–60.

(41) Froberg MK, Gerhart DZ, Enerson BE, Manivel C, Guzman-Paz M, Seacotte N, *et al.* Expression of monocarboxylate transporter MCT1 in normal and neoplastic human CNS tissues. *Neuroreport* **2001**;12:761–5.

(42) Lee GH, Kim DS, Chung MJ, Chae SW, Kim HR, Chae HJ. Lysyl oxidase-like-1 enhances lung metastasis when lactate accumulation and monocarboxylate transporter expression are involved. *Oncol Lett* **2011**;2:831–8.

(43) Gatenby RA, Gawlinski ET, Gmitro AF, Kaylor B, Gillies RJ. Acid-mediated tumor invasion: a multidisciplinary study. *Cancer Res* **2006**;66:5216–23.

(44) Newell K, Franchi A, Pouyssegur J, Tannock I. Studies with glycolysis-deficient cells suggest that production of lactic acid is not the only cause of tumor acidity. *Proc Natl Acad Sci U S A* **1993**;90:1127–31.

(45) Becker HM, Hirnet D, Fecher-Trost C, Sultemeyer D, Deitmer JW. Transport activity of MCT1 expressed in Xenopus oocytes is increased by interaction with carbonic anhydrase. *J Biol Chem* **2005**;280:39882–9.

(46) Slomiany MG, Grass GD, Robertson AD, Yang XY, Maria BL, Beeson C, *et al.* Hyaluronan, CD44, and emmprin regulate lactate efflux and membrane localization of monocarboxylate transporters in human breast carcinoma cells. *Cancer Res* **2009**;69:1293–301.

(47) Noor SI, Dietz S, Heidtmann H, Boone CD, McKenna R, Deitmer JW, *et al.* Analysis of the binding moiety mediating the interaction between monocarboxylate transporters and carbonic anhydrase II. *J Biol Chem* **2015**;290:4476–86.

Downloaded from cancerres.aacrjournals.org on September 20, 2017. © 2017 American Association for Cancer Research.

Author Manuscript Published OnlineFirst on August 21, 2017; DOI: 10.1158/0008-5472.CAN-17-0764
Author manuscripts have been peer reviewed and accepted for publication but have not yet been edited.

(48) Kennedy KM, Dewhirst MW. Tumor metabolism of lactate: the influence and therapeutic potential for MCT and CD147 regulation. *Future Oncol* **2010**;6:127–48.

(49) Venkatesan B, Valente AJ, Prabhu SD, Shanmugam P, Delafontaine P, Chandrasekar B. EMMPRIN activates multiple transcription factors in cardiomyocytes, and induces interleukin-18 expression via Rac1-dependent PI3K/Akt/IKK/NF-kappaB andMKK7/JNK/AP-1 signaling. *J Mol Cell Cardiol* **2010**;49:655–63.

(50) Zhai Y, Wu B, Li J, Yao XY, Zhu P, Chen ZN. CD147 promotes IKK/IkappaB/NF-kappaB pathway to resist TNF-induced apoptosis in rheumatoid arthritis synovial fibroblasts. *J Mol Med (Berl)* **2016**;94:71–82.

Downloaded from cancerres.aacrjournals.org on September 20, 2017. © 2017 American Association for Cancer Research.

Author Manuscript Published OnlineFirst on August 21, 2017; DOI: 10.1158/0008-5472.CAN-17-0764
Author manuscripts have been peer reviewed and accepted for publication but have not yet been edited.

Legends of the Figures

Figure 1. *MCT1* silencing or deletion decreases cancer cell migration and invasion. A-B, *MCT1* was silenced in SiHa cancer cells using siRNA (SiHa-siMCT1), shRNA (SiHa-shMCT1) or deleted using a CRISPR-Cas9 strategy (SiHa-CRISPR-MCT1). **A,** Comparative migration of SiHa-siCTR *versus* SiHa-siMCT1 (*left*, *n* = 8), SiHa-shCTR *versus* SiHa-shMCT1 (*middle*, *n* = 11-12) and in SiHa-WT *versus* SiHa-CRISPR-MCT1 (*right*, *n* = 6) in a Boyden chamber with 0.15% FBS as chemoattractant. Upper panels show representative pictures (bars = 100 µm). **B,** Comparative invasion of SiHa-shCTR *versus* SiHa-shMCT1 (*left*, *n* = 6) and in SiHa WT *versus* SiHa-CRISPR-MCT1 (*right*, *n* = 8) in a Boyden chamber with 5% FBS as chemoattractant. Upper panels show representative pictures (bars = 100 µm). **C-D,** *MCT1* was silenced in 4T1 mouse mammary carcinoma cells using 2 different shRNAs (4T1-shMCT1a and 4T1-shMCT1b). **C,** Cell migration in a Boyden chamber (*n* = 16). Upper panels show representative pictures (bars = 100 µm). **D,** Cell invasion in a Boyden chamber (*n* = 25-26). Upper panels show representative pictures (bars = 100 µm). ** $P < 0.01$, *** $P < 0.005$; by Student's *t* test (**A, B**) or by one-way ANOVA with Dunnett's post-hoc test (**C, D**).

Figure 2. *MCT1* silencing or deletion decreases lactic acid efflux from SiHa and 4T1 cells. A-F, *MCT1* was silenced in SiHa cancer cells using shRNA (SiHa-shMCT1) or deleted using CRISPR-Cas9 (SiHa-CRISPR-MCT1). **A,** Glucose consumption by SiHa-shCTR *versus* SiHa-shMCT1 (*left*, *n* = 6) and in SiHa WT *versus* SiHa-CRISPR-MCT1 (*right*, *n* = 5-6). **B,** Lactate release by SiHa-shCTR *versus* SiHa-shMCT1 (*left*, *n* =

Downloaded from cancerres.aacrjournals.org on September 20, 2017. © 2017 American Association for Cancer Research.

Author Manuscript Published OnlineFirst on August 21, 2017; DOI: 10.1158/0008-5472.CAN-17-0764
Author manuscripts have been peer reviewed and accepted for publication but have not yet been edited.

6) and in SiHa WT *versus* SiHa-CRISPR-MCT1 (*right*, *n* = 5-6). **C,** Glycolytic extracellular acidification rate (ECAR) measured with a Seahorse analyzer in SiHa-shCTR *versus* SiHa-shMCT1 (*left*, *n* = 15) and in SiHa WT *versus* SiHa-CRISPR-MCT1 (*right*, *n* = 7-8). **D,** Oxygen consumption rate (OCR) measured with a Seahorse analyzer in SiHa-shCTR *versus* SiHa-shMCT1 (*left*, *n* = 13-15) and in SiHa WT *versus* SiHa-CRISPR-MCT1 (*right*, *n* = 7-8). **E,** Basal mitochondrial OCR calculated from D. **F,** Maximal mitochondrial OCR calculated from D. **G-J,** *MCT1* was silenced using 2 different shRNAs in 4T1-shMCT1a and 4T1-shMCT1b cells. **G,** Glucose consumption (*n* = 3). **H,** Lactate release (*n* = 3). **I,** Glycolytic ECAR (*n* = 7). **J,** OCR, basal mitochondrial OCR and maximal mitochondrial OCR (*n* = 7). *ns* $P > 0.05$, * $P < 0.05$, *** $P < 0.005$; by Student's *t* test (**A-F**) or one-way ANOVA with Dunnett's post-hoc test (**G-J**).

Figure 3. Pharmacological MCT1 inhibition decreases lactic acid efflux but does affect cancer cell migration and invasion. A-I, MCT1 activity was inhibited in cancer cells by AR-C155858 or AZD3965. Vehicle was 0.1% DMSO. **A,** Glucose consumption by SiHa-WT cells treated with AR-C155858 (*left*, *n* = 8-9) or AZD3965 (*right*, *n* = 5-6) *versus* vehicle. **B,** Lactate release by SiHa-WT cells treated with AR-C155858 (*left*, *n* = 8-9) or AZD3965 (*right*, *n* = 5-6) *versus* vehicle. **C,** Glycolytic extracellular acidification rate (ECAR) of SiHa-WT cells (*n* = 6). **D,** SiHa-WT cell migration when treated with AR-C155858 (*left*, *n* = 15) or AZD3965 (*right*, *n* = 12) *versus* vehicle in a Boyden Chamber. Upper panels show representative pictures (bars = 100 µm). **E,** SiHa WT cell invasion in a Boyden Chamber (*n* = 10). Upper panels show representative pictures (bars = 100 µm). **F,** Glucose consumption of 4T1 cells (*n* = 6). **G,** Lactate release by 4T1 cells (*n* = 6). **H,** 4T1 cell migration (*n* = 12). Upper panels show representative pictures (bars =

Downloaded from cancerres.aacrjournals.org on September 20, 2017. © 2017 American Association for Cancer Research.

Author Manuscript Published OnlineFirst on August 21, 2017; DOI: 10.1158/0008-5472.CAN-17-0764
Author manuscripts have been peer reviewed and accepted for publication but have not yet been edited.

100 µm). **I,** 4T1 cell invasion (*n* = 12). Upper panels show representative pictures (bars = 100 µm). **J,** Migration of 4T1 cells silenced for *MCT1* (shMCT1a) and expressing or not wild-type human MCT1 (hMCT1^{+}) (*n* = 8). Western blots show MCT1 and β-actin expression (*n* = 3). Upper panels show representative pictures (bars = 100 µm). **K,** Migration of SiHa cells deleted for *MCT1* using CRISPR-Cas9 (SiHa-CRISPR-MCT1) and expressing or not mutated/inactive human MCT1 (hMCT1^{-}) (*n* = 12). Western blots show MCT1 and HSP-90 expression (*n* = 2). Upper panels show representative pictures (bars = 100 µm). *ns* $P > 0.05$, * $P < 0.05$, ** $P < 0.01$, *** $P < 0.005$; by one-way ANOVA with Dunnett's post-hoc test (**A-B** *left*) or by Student's *t* test (**A-B** *right*, **C-K**).

Figure 4. Superinvasive SiHa-F3 and SiHa-ρ0 cells have high MCT1 expression that promotes migration and invasion. A-F, Where indicated, *MCT1* was silenced using siMCT1 or shMCT1. **A,** Representative western blots of MCT1, MCT4, CD147 and HSP-90 expression. **B,** SiHa-F3 migration (*left*, *n* = 4) and invasion (*right*, *n* = 17-18) in Boyden chambers. Upper panels show representative pictures (bars = 100 µm). **C,** SiHa-F3 migration (*left*, *n* = 10) and invasion (*right*, *n* = 12) upon treatment with 10 µM of AR-C155858 or vehicle. Upper panels show representative pictures (bars = 100 µm). **D,** Representative western blots of MCT1, MCT4, CD147 and β-actin expression. **E,** SiHa-ρ0 migration (*left*, *n* = 4) and invasion (*right*, *n* = 8). Upper panels show representative pictures (bars = 100 µm). *ns* $P > 0.05$, * $P < 0.05$, *** $P < 0.005$ *versus* control; $^{\#\#\#}$ $P < 0.005$ *versus* SiHa-F3-shCTR; $^{\$\$\$}$ $P < 0.005$ *versus* SiHa-ρ0-siCTR; by one-way ANOVA with Dunnett's post-hoc test (**B** *left***, E** *left*) or Student's *t* test (**B** *right***, C, E** *right*).

Downloaded from cancerres.aacrjournals.org on September 20, 2017. © 2017 American Association for Cancer Research.

Author Manuscript Published OnlineFirst on August 21, 2017; DOI: 10.1158/0008-5472.CAN-17-0764
Author manuscripts have been peer reviewed and accepted for publication but have not yet been edited.

Figure 5. NF-κB controls MCT1-dependent cancer cell migration. A, Comparison of phospho-Ser536-p65, total p65 and HSP-90 protein expression in SiHa-shCTR *versus* SiHa-shMCT1 (*n* = 6) and SiHa-WT *versus* SiHa-CRISPR-MCT1 (*n* = 9). **B,** Representative blots of IκKα, IκKβ and HSP-90 in SiHa-WT and SiHa-CRISPR-MCT1 cells (*n* = 6-12). **C,** Comparison of phospho-Ser536-p65, total p65 and β-actin protein expression in 4T1-shCTR versus 4T1-shMCT1a and 4T1-shMCT1b cells (*n* = 9). **D,** Migration in a Boyden chamber of SiHa-CRISPR-MCT1 cells pretreated for 2 h ± TNFα (*left*, *n* = 12) or TPA (*right*, *n* = 15) with or without NF-κB inhibitor BMS-345541. Upper panels show representative pictures (bars = 100 µm). **E,** Migration in a Boyden chamber of SiHa-WT and SiHa-CRISPR-MCT1 cells pretreated for 24 h and treated during the assay ± BMS-345541 (*n* = 8). Upper panels show representative pictures (bars = 100 µm). *ns* $P > 0.05$, * $P < 0.05$, ** $P < 0.01$, *** $P < 0.005$ *versus* first column or as indicated; $^{\#}$ $P < 0.05$, $^{\#\#}$ $P < 0.01$ *versus* second column; by Student's *t* test (**A**) or one-way ANOVA with Dunnett's (**C-D**) or Bonferroni's (**E**) post-hoc test.

Figure 6. *MCT1* silencing decreases spontaneous 4T1 metastasis. Spontaneous lung metastasis assay using luciferase-expressing 4T1-shCTR, 4T1-shMCT1a and 4T1-shMCT1b cancer cells that were implanted subcutaneously to form primary tumors in immunocompetent syngeneic mice. Lungs were analyzed 38 days after primary tumor implantation. **A,** Representative pictures and quantification of the luciferase signal in mouse lungs (*n* = 8-9). **B,** Quantification of the number of surface metastases in mouse lungs (*n* = 8-9). **C,** Representative micrographs of H&E-stained lung sections where metastasis are indicated with an asterisk and quantification of the number of metastases

Downloaded from cancerres.aacrjournals.org on September 20, 2017. © 2017 American Association for Cancer Research.

Author Manuscript Published OnlineFirst on August 21, 2017; DOI: 10.1158/0008-5472.CAN-17-0764
Author manuscripts have been peer reviewed and accepted for publication but have not yet been edited.

(*left*) and metastatic area (*right*) normalized to lung area (n = 8-9). * $P < 0.05$, ** $P < 0.01$, *** $P < 0.005$; by one-way ANOVA with Dunnett's post-hoc test (**A-C**).

Downloaded from cancerres.aacrjournals.org on September 20, 2017. © 2017 American Association for Cancer Research.

Author Manuscript Published OnlineFirst on August 21, 2017; DOI: 10.1158/0008-5472.CAN-17-0764
Author manuscripts have been peer reviewed and accepted for publication but have not yet been edited.

Figure 1

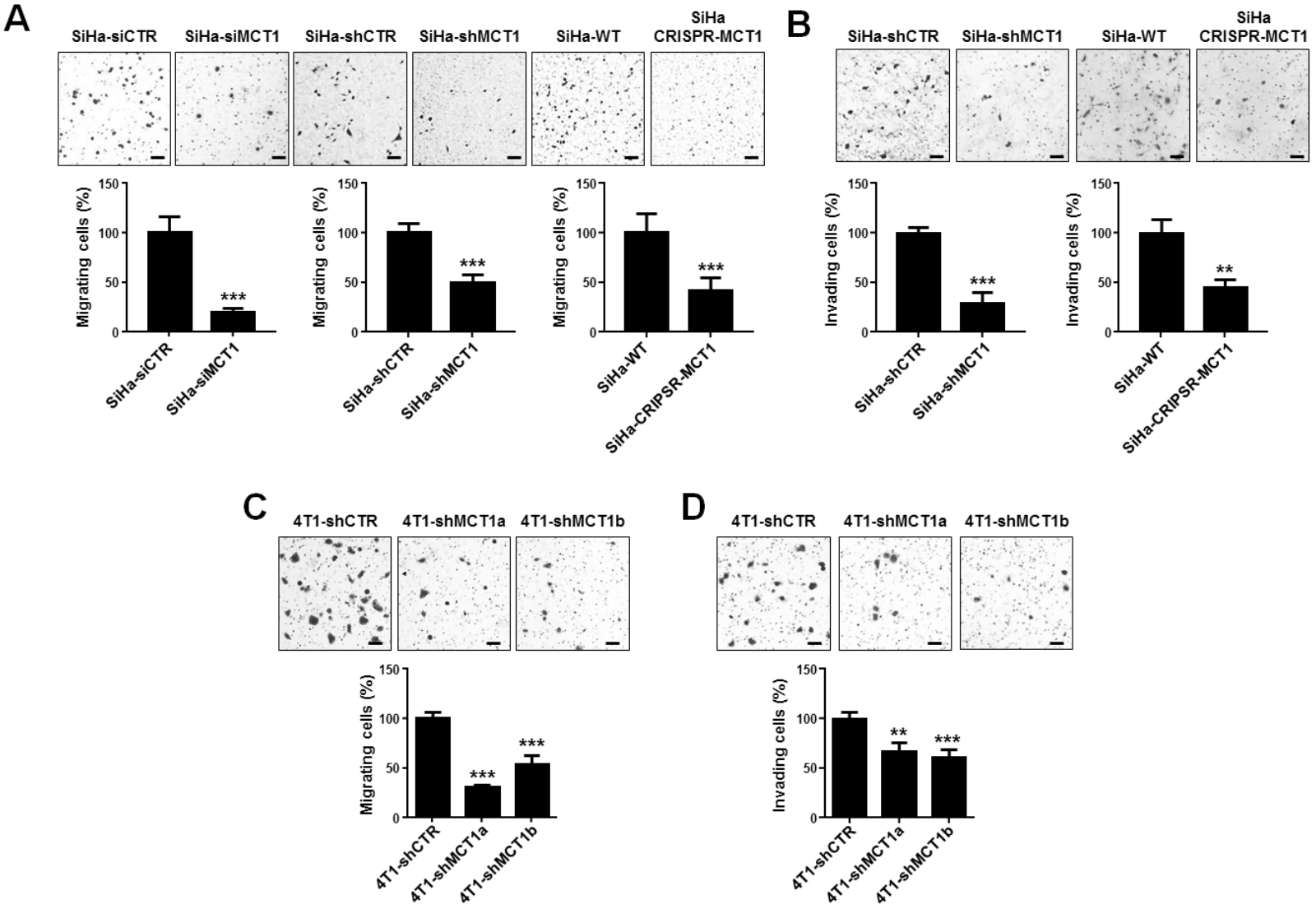

Downloaded from cancerres.aacrjournals.org on September 20, 2017. © 2017 American Association for Cancer Research.

Author Manuscript Published OnlineFirst on August 21, 2017; DOI: 10.1158/0008-5472.CAN-17-0764
Author manuscripts have been peer reviewed and accepted for publication but have not yet been edited.

Figure 2

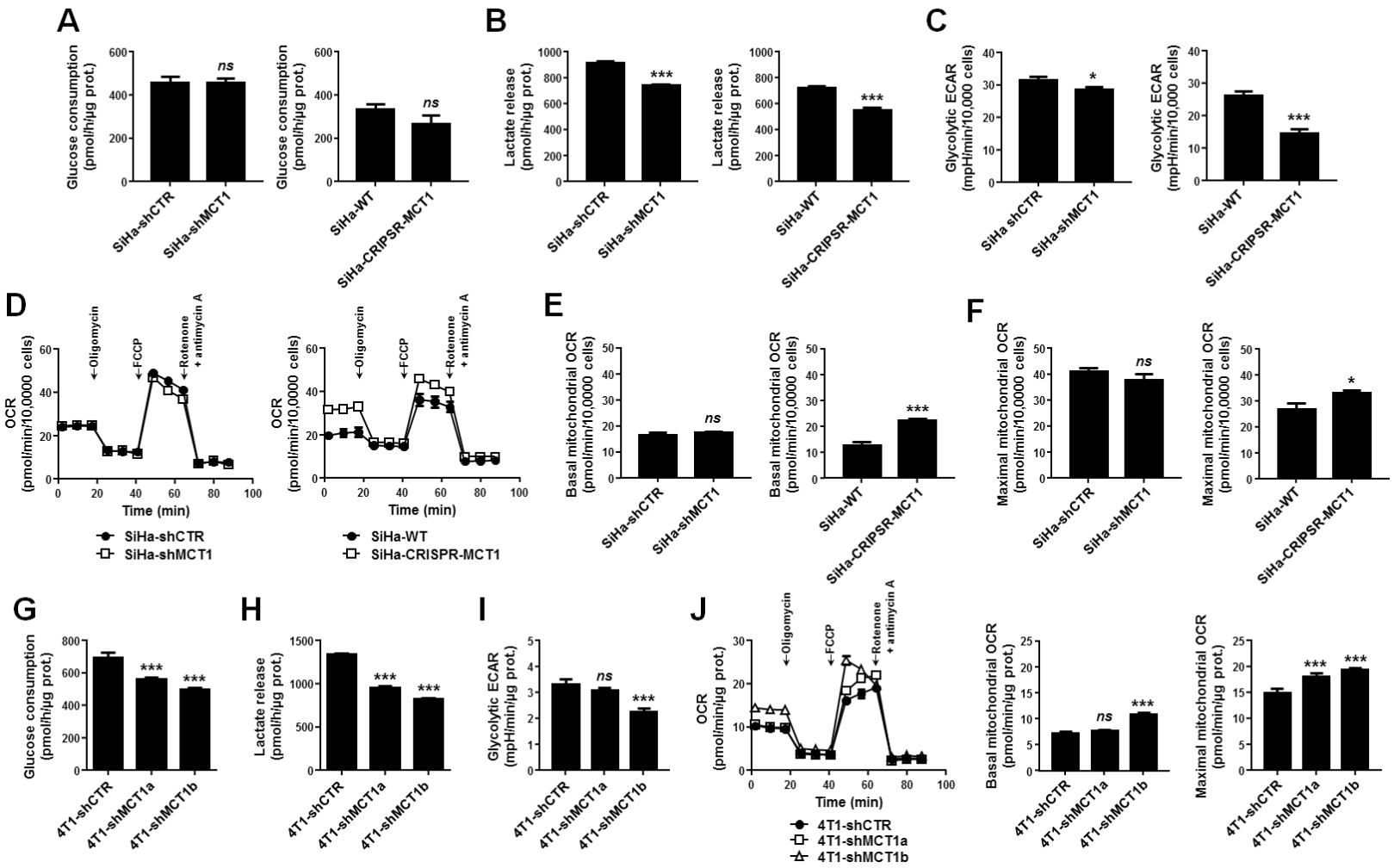

Downloaded from cancerres.aacrjournals.org on September 20, 2017. © 2017 American Association for Cancer Research.

Author Manuscript Published OnlineFirst on August 21, 2017; DOI: 10.1158/0008-5472.CAN-17-0764
Author manuscripts have been peer reviewed and accepted for publication but have not yet been edited.

Figure 3

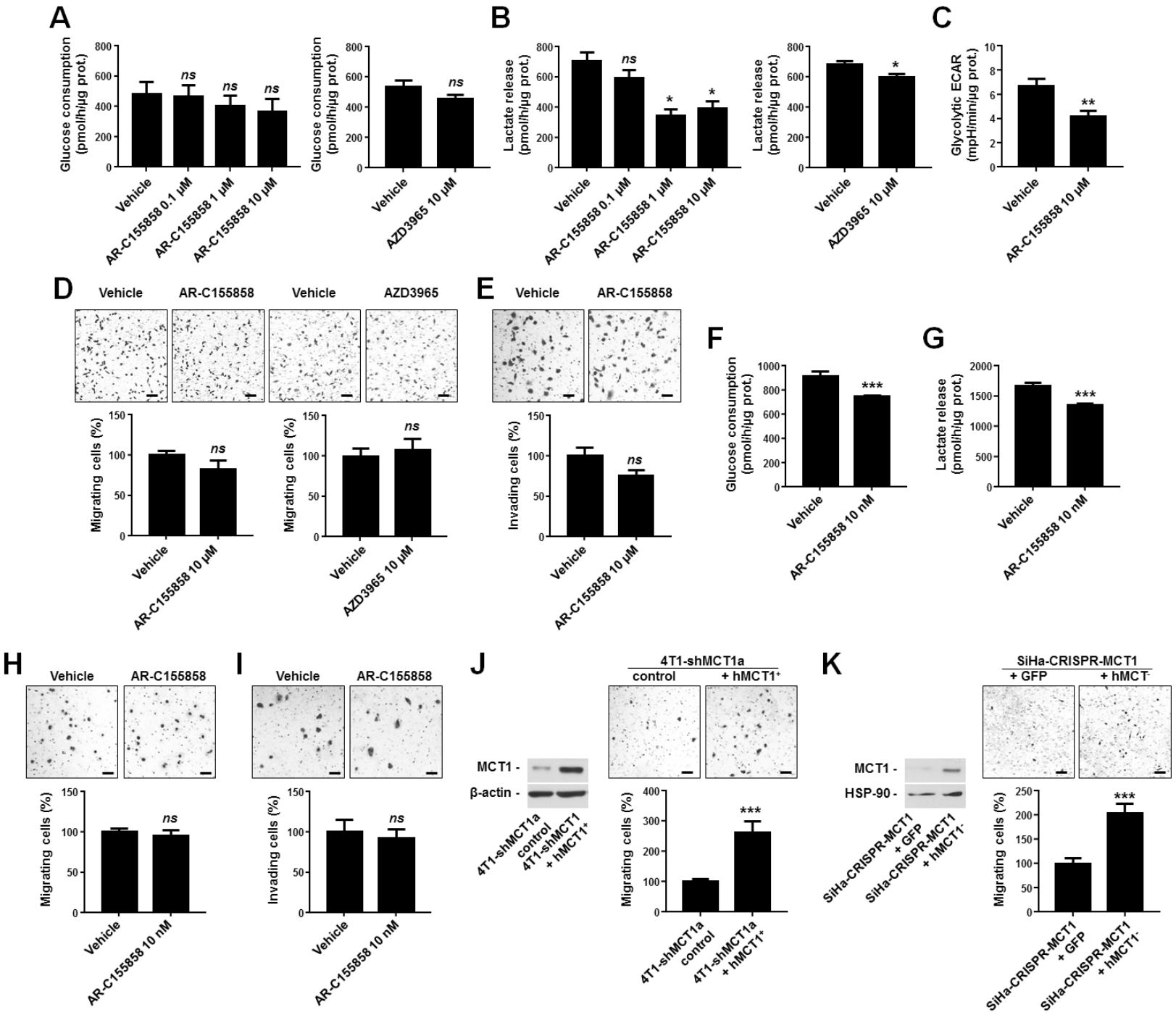

Downloaded from cancerres.aacrjournals.org on September 20, 2017. © 2017 American Association for Cancer Research.

Author Manuscript Published OnlineFirst on August 21, 2017; DOI: 10.1158/0008-5472.CAN-17-0764
Author manuscripts have been peer reviewed and accepted for publication but have not yet been edited.

Figure 4

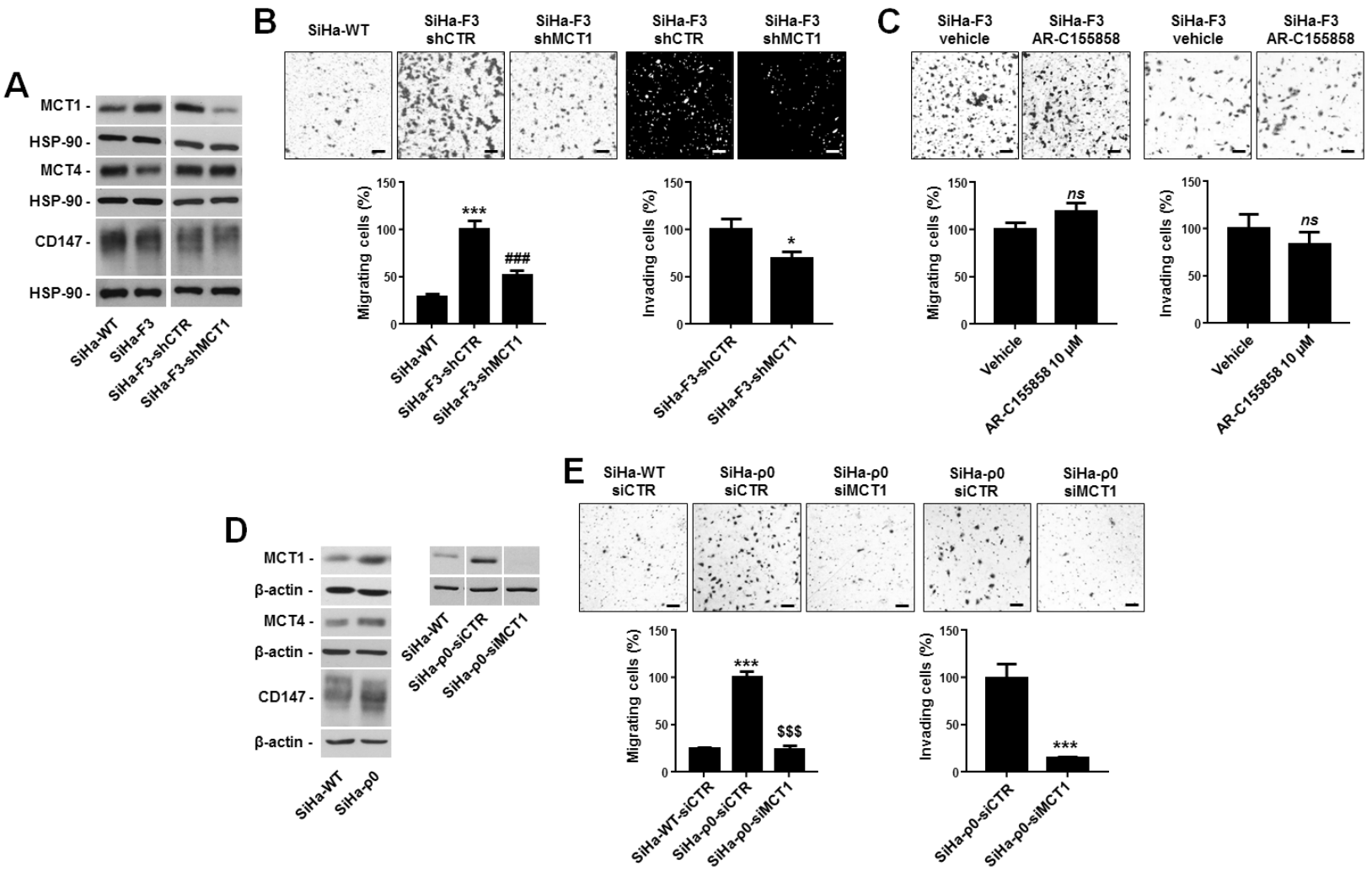

Downloaded from cancerres.aacrjournals.org on September 20, 2017. © 2017 American Association for Cancer Research.

Author Manuscript Published OnlineFirst on August 21, 2017; DOI: 10.1158/0008-5472.CAN-17-0764
Author manuscripts have been peer reviewed and accepted for publication but have not yet been edited.

Figure 5

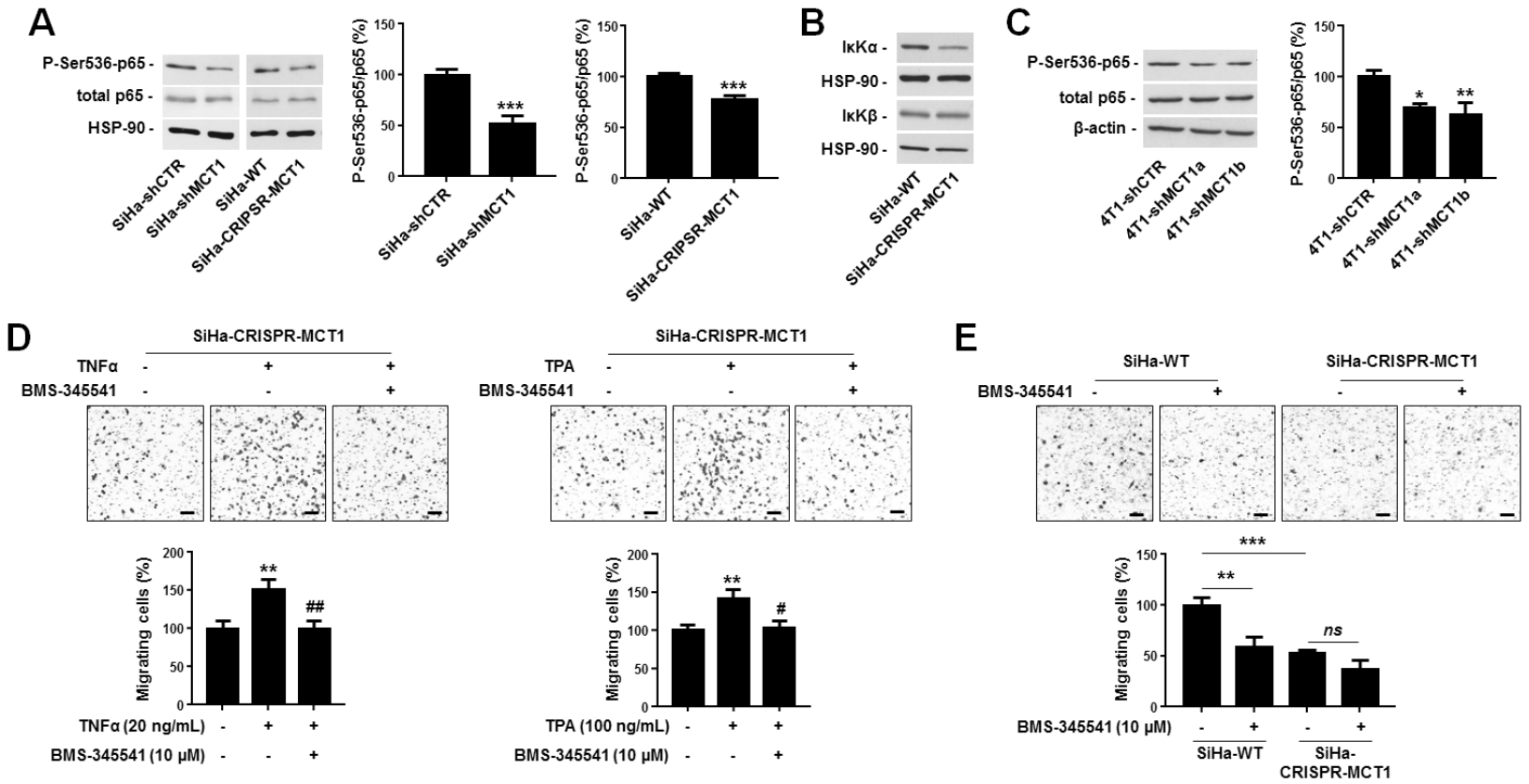

Downloaded from cancerres.aacrjournals.org on September 20, 2017. © 2017 American Association for Cancer Research.

Author Manuscript Published OnlineFirst on August 21, 2017; DOI: 10.1158/0008-5472.CAN-17-0764
Author manuscripts have been peer reviewed and accepted for publication but have not yet been edited.

Figure 6

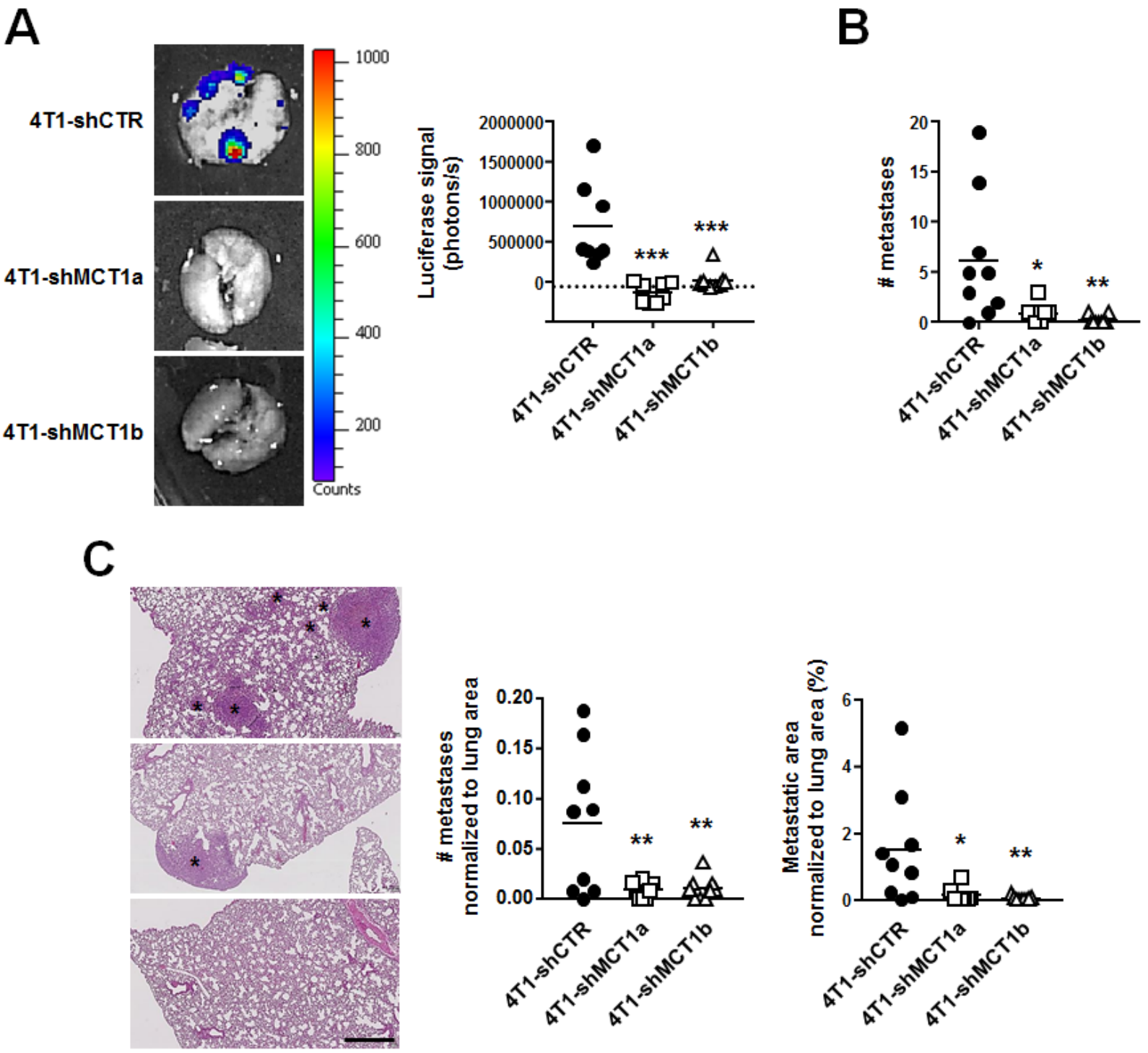

Downloaded from cancerres.aacrjournals.org on September 20, 2017. © 2017 American Association for Cancer Research.

Author Manuscript Published OnlineFirst on August 21, 2017; DOI: 10.1158/0008-5472.CAN-17-0764
Author manuscripts have been peer reviewed and accepted for publication but have not yet been edited.

Cancer Research
The Journal of Cancer Research (1916–1930) | The American Journal of Cancer (1931–1940)

AACR American Association for Cancer Research

Monocarboxylate transporter MCT1 promotes tumor metastasis independently of its activity as a lactate transporter

Valéry L Payen, Myriam Y Hsu, Kristin S Rädecke, et al.

Cancer Res Published OnlineFirst August 21, 2017.

Updated version	Access the most recent version of this article at: doi:10.1158/0008-5472.CAN-17-0764
Supplementary Material	Access the most recent supplemental material at: http://cancerres.aacrjournals.org/content/suppl/2017/08/18/0008-5472.CAN-17-0764.DC1
Author Manuscript	Author manuscripts have been peer reviewed and accepted for publication but have not yet been edited.

E-mail alerts	Sign up to receive free email-alerts related to this article or journal.
Reprints and Subscriptions	To order reprints of this article or to subscribe to the journal, contact the AACR Publications Department at pubs@aacr.org.
Permissions	To request permission to re-use all or part of this article, contact the AACR Publications Department at permissions@aacr.org.

Downloaded from cancerres.aacrjournals.org on September 20, 2017. © 2017 American Association for Cancer Research.